



# The effect of contamination on the bubble cluster formation in swarm of spherical bubbles rising along an inclined flat wall



Toshiyuki Ogasawara\*, Hiroyuki Takahira

Department of Mechanical Engineering, Osaka Prefecture University, Japan

## ARTICLE INFO

### Keywords:

Bubble cluster  
Inclined flat wall  
Clean bubble  
Fully-contaminated bubble

## ABSTRACT

The motion of mono-dispersed spherical bubbles rising along an inclined flat wall is investigated experimentally. An inclination angle of the flat wall is changed to control the bubble Reynolds number set to be 100. As an experimental condition, the boundary condition on the bubble surface (free-slip and no-slip conditions) is controlled, and its effect on the motion of the bubbles has been analyzed.  $\text{MgSO}_4$  solution and Triton X-100 solution are used to achieve free-slip and no-slip bubble surfaces, respectively. Bubble coalescences are almost inhibited by using these additives. The bubbles tend to be horizontally arranged in lines and such arrangements pile up to be remarkable bubble clusters. The radial pair distribution function and the conditional average of the relative velocity of two bubbles are calculated to evaluate the spatial distribution and bubble–bubble interaction quantitatively. The results show that the tandem configuration of bubble pair next to each other frequently appears due to the increment in the rising velocity of the trailing bubble; a horizontally-oriented (side-by-side) configuration is stable compared to a vertically-oriented (tandem) one, which leads to a horizontally arranged bubbles in a single line. A similar tendency for the bubble clustering is confirmed for both free-slip bubbles and no-slip bubbles. However, there are some quantitative differences such as the faster approaching velocity of the trailing bubble in wider wake region of the leading bubble for no-slip bubbles, etc. The bubble cluster velocity as a velocity of highly accumulated bubbles is also defined and evaluated.

## 1. Introduction

Bubbly flows are found in many industrial fields in which bubbles enhance mixing and heat and mass exchanges due to the larger interfacial area and the agitation effect. Bubble-bubble interaction is fundamental physics in bubbly flow, and a general understanding of the interaction and its effect on the whole structure of the bubbly flow is necessary. One of the interesting phenomena as a result of the bubble-bubble interaction is a clustering behavior of bubbles. The bubble clustering gives non-uniform distribution of the buoyancy force in the bubbly flow and affects the macroscopic flow structure (Takagi and Matsumoto, 2011).

A disk-like shaped bubble cluster in a homogeneous bubble swarm due to the potential interaction is predicted by the analytical and numerical studies (Sangani and Didwania, 1993; Smereka, 1993). At moderate bubble Reynolds number, some numerical simulations have reported bubble clusters which are formed by less-deformed nearly-spherical bubbles (Bunner and Tryggvason, 2002; Esmaeli and Tryggvason, 2005). The bubble-bubble interaction have been investigated numerically for tandem configuration (Yuan and Prosperetti,

1994), side-by-side configuration (Legendre et al., 2003) and any orientation (Hallez and Legendre, 2011), which are closely related to the cluster formation. There are experimental studies trying to reproduce the bubble cluster, and the mild clustering behavior has been reported (Zenit et al., 2001; Figueroa-Espinoza and Zenit, 2005). However, because of the difficulties in the experiment such as the agitation effect of bubbles at high Reynolds number, the perfect reproduction of the bubble cluster due to the potential interaction has not been achieved yet. At the intermediate bubble Reynolds number of from 5 to 75, a separating velocity between side-by-side bubbles which increases with increase in the bubble Reynolds number has been shown by the experiment (Murai et al., 2006).

Not only for a bubble swarm in bulk but also for sliding bubbles along the inclined flat wall, the bubble-bubble interaction and the clustering of the clean bubbles have been investigated experimentally. Kitagawa et al. (2004) showed the bubble configuration of the nearest bubble pair changes from tandem to side-by-side with increase in the bubble Reynolds number from 1 to 15. Ogasawara et al. (2016) investigated the sliding bubble along the inclined wall at the bubble Reynolds number of from 100 to 200 in the clean system, and showed

\* Corresponding author at: 1-1 Gakuen-cho, Naka-ku, Sakai-shi, Osaka 599-8531, Japan.  
E-mail address: [oga@me.osakafu-u.ac.jp](mailto:oga@me.osakafu-u.ac.jp) (T. Ogasawara).

horizontally aligned bubbles and remarkable bubble clusters. The same type of this bubble cluster which is formed by mono-dispersed spherical bubbles rising along vertical walls in upward channel flow due to the shear-induced lift force in the presence of surfactants has been also reported (Takagi et al., 2008). In these cases, two-dimensional constraint on the bubble motion is an important factor. However, the effect of the surfactant, which causes Marangoni effect and changes the boundary condition of the bubble surface, on the clustering behavior is not understood well. For practical applications, the effect of these impurities in water such as surfactant and/or electrolyte becomes important.

Therefore, the objective of this study is to investigate the effect of the boundary condition of the bubble surface on the motion of mono-dispersed spherical bubbles rising along an inclined flat wall at the bubble Reynolds number of 100. Since these bubbles keep a spherical shape and slide up along the wall without leaping motion, the bubble motion is restricted two-dimensionally due to the presence of the inclined wall. The development of the bubble cluster is also investigated.

## 2. Experimental setup

### 2.1. Experimental apparatus and conditions

The experimental apparatus is shown in Fig. 1. To achieve the bubbles sliding along an inclined flat wall, an inclined rectangular channel is used. The channel is made of acrylic resin and its size is 980 mm in height, 300 mm in width and 40 mm in depth. The channel is designed to have sufficiently long depth so as not to give any influences of the lower wall on the bubbles rising along the upper wall. The inclination angle of the channel  $\theta$  can be changed from 90 deg. (vertical) to 15 deg. Bubbles are generated from 40 stainless steel capillary tubes (inner diameter of 100  $\mu\text{m}$ ) arranged in a line with 5 mm intervals. Air is used as a gas phase. 0.1 M  $\text{MgSO}_4$  aqueous solution and 10 ppm Triton X-100 aqueous solution are used as a liquid phase to avoid bubble coalescence. In 10 ppm Triton X-100 solution, surfactant causes so-called Marangoni effect and the bubble surface almost becomes no-slip condition, so that the bubble becomes fully-contaminated. On the other hand, in electrolyte solution (0.1 M  $\text{MgSO}_4$  solution), the surface tension of air–water interface increases a little bit, however, Marangoni effect does not occur and the bubble surface keeps the free-slip boundary condition. Therefore, the bubbles in 0.1 M  $\text{MgSO}_4$  solution can be regarded as clean bubbles. To avoid the contaminations due to remained solutes, the channel is washed by tap water twice and is rinsed by distilled water once after every experiment. The drag coefficients of 1 mm bubble are also evaluated from the terminal velocities in the bulk solutions at rest which are the same as those used in the present experiments, and we have confirmed that the drag coefficients in  $\text{MgSO}_4$  aqueous solution and in Triton X-100 solution become almost the same as those for a clean spherical bubble (Mei

et al., 1994) and for a rigid sphere (Clift et al., 1978), respectively. The gas flow rate  $Q_g$  is controlled by a mass flow controller and set to be 50 ml/min. Although this gas flow rate  $Q_g$  certainly influences the bubbles' motion, this dependence is out of focus in the present study. To analyze the development of the bubble cluster as it rises, three test sections are set at 150 mm, 350 mm and 550 mm above the bubble generation point along the wall (This distance from the bubble generation point to each test section is indicated by  $L$ ). The size of the measurement window at each test section is 90 mm square. The shadow images of the bubbles are recorded by high-speed video camera at 250 frames per second for the bubbles' motion observation and at 2 frames per second for the bubble size measurement.  $x$ - $y$  plane is set on the wall;  $x$  denotes the horizontal direction and  $y$  denotes the upward direction in which the bubble rises along the wall.

### 2.2. Detection of bubble centers and radii

It is necessary to detect the bubble centers and radii from captured bubble images to evaluate quantitatively the spatial distribution of bubbles, the behaviors of bubbles and bubble clusters. In the present experimental arrangement, the bubbles distribute two-dimensionally in the wall vicinity, hence bubble images do not overlap each other. However, there exist adjacent bubbles attaching on their edges, which make it difficult to detect each single bubble by the image processing using the binarization method. To overcome this problem, Hough transformation method (Davies, 2005) is utilized to detect the bubble centers and corresponding radii. The velocity vectors of the bubbles are calculated by taking backward difference of the positions of the tracked bubble centers with a time interval of 1/250 s.

## 3. Results and discussion

### 3.1. Bubble cluster

Rising velocities of clean bubble and contaminated bubble are different with each other because the imposed boundary conditions on the bubble surface are free-slip and no-slip conditions, respectively. In the present experiment, the component of the buoyancy force along the wall is controllable by changing the inclination angle of the channel  $\theta$ , which enables to change bubble Reynolds number  $Re$  in the experiment. Now,  $Re$  is defined as  $Re = dV/\nu$ , where  $d$ ,  $V$  and  $\nu$  denote the mean bubble diameter, the average rising velocity along the wall and the kinematic viscosity in each condition, respectively. In this experiment,  $Re$  takes the value of almost 100 at  $\theta = 30$  deg. in 0.1 M  $\text{MgSO}_4$  aq. and  $\theta = 40$  deg. in 10 ppm Triton X-100 aq. ( $Q_g = 50$  ml/min and  $L = 350$  mm). From now on, the results under these two conditions are shown to compare the effect of free-slip and no-slip boundary conditions of the bubble surface at the same  $Re$  of 100. Although the  $Re$  number is the same, the normal component of the buoyancy force acting on the bubble differs in the cases of free-slip and no-slip conditions because the inclination angle differs in each case. It is unknown to what extent this difference affects the bubble-bubble interaction and/or whether it is negligible or not.

Fig. 2 shows snapshots of bubbles at different test sections  $L = 150$  mm, 350 mm and 550 mm. For both free-slip bubbles and no-slip bubbles, mono-dispersed spherical bubbles are obtained. Fig. 3 shows bubble diameter distributions for free-slip bubbles (0.1 M  $\text{MgSO}_4$  aq.,  $\theta = 30$  deg.,  $Q_g = 50$  ml/min) and for no-slip bubbles (10 ppm Triton X-100 aq.,  $\theta = 40$  deg.,  $Q_g = 50$  ml/min) at  $L = 350$  mm. Both distributions have major peaks around 1.3 mm. Also weak peaks can be seen around 1.6 mm, which correspond to the bubble diameter after the coalescence ( $1.6 \sim 2^{1/3} \times 1.3$ ). The standard deviations are less than 0.1 mm. Bubble coalescences occasionally occur while the bubbles rise. It is confirmed from the observation that, although the number of coalesced bubbles is small at every test section, it increases as the distance from the bubble generation point  $L$  becomes larger. The effect of

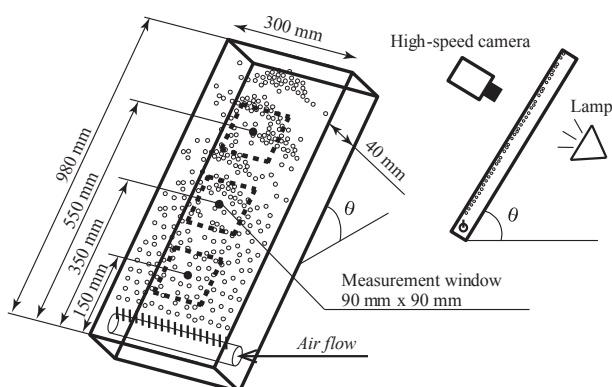


Fig. 1. Experimental apparatus.

Download English Version:

<https://daneshyari.com/en/article/6758621>

Download Persian Version:

<https://daneshyari.com/article/6758621>

[Daneshyari.com](https://daneshyari.com)